Supplemental Material for

Sequence-based correction of barcode bias in massively parallel reporter assays

Dongwon Lee[1,5*], Ashish Kapoor[2], Changhee Lee[3], Michael Mudgett[4], Michael A. Beer[4], Aravinda Chakravarti[1]

*Corresponding author: dongwon.lee@childrens.harvard.edu

This document includes:

Supplemental Figures S1 to S10

Supplemental Tables S1 to S8

Supplemental Notes

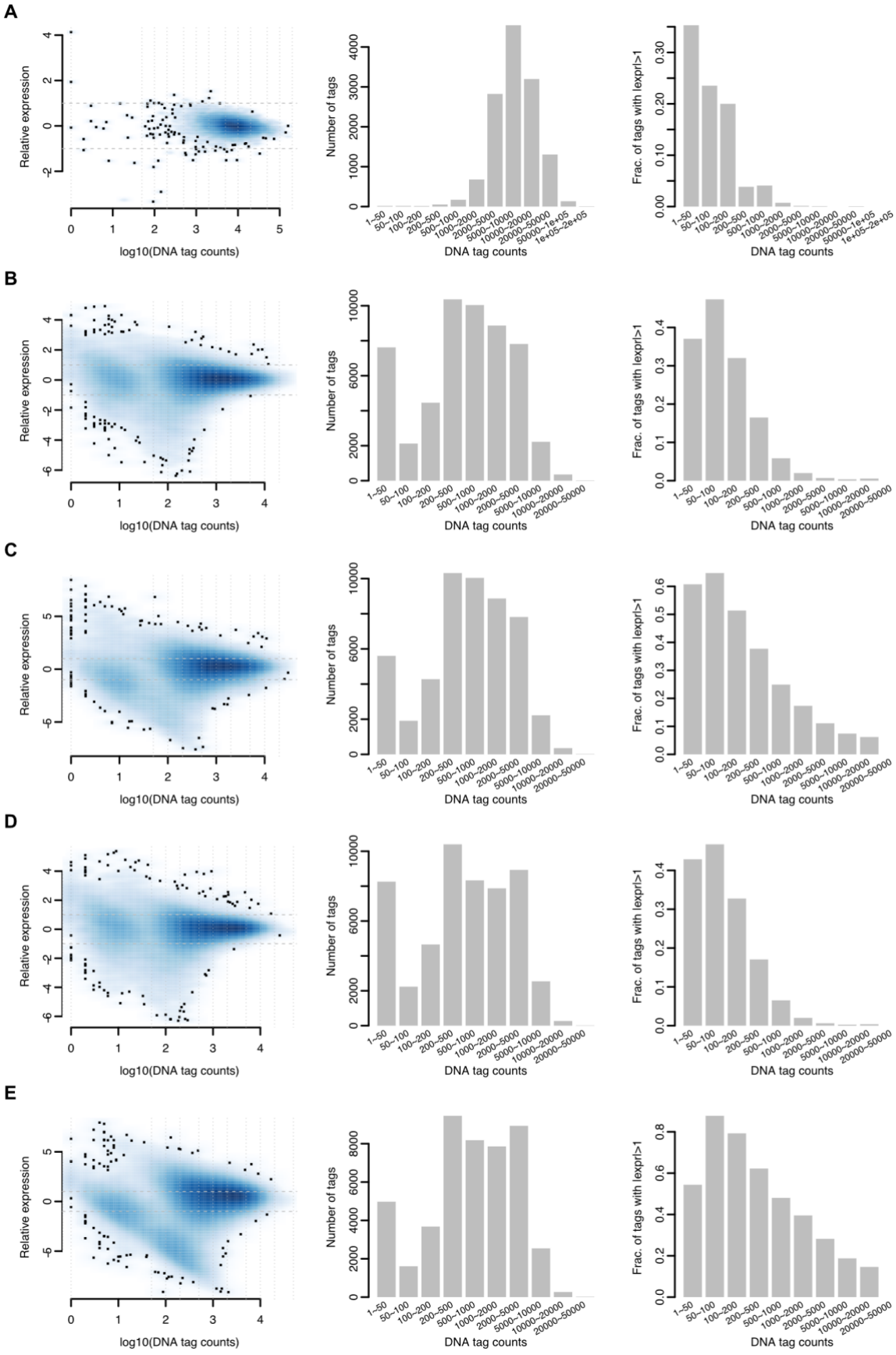
A
B
C
D
E
Relative expression
log10(DNA tag counts)
Number of tags
DNA tag counts
Frac. of tags with lexpr|>1
1~50
50~100
100~200
200~500
500~1000
1000~2000
2000~5000
5000~10000
10000~20000
20000~50000
50000~1e+05
1e+05~2e+05

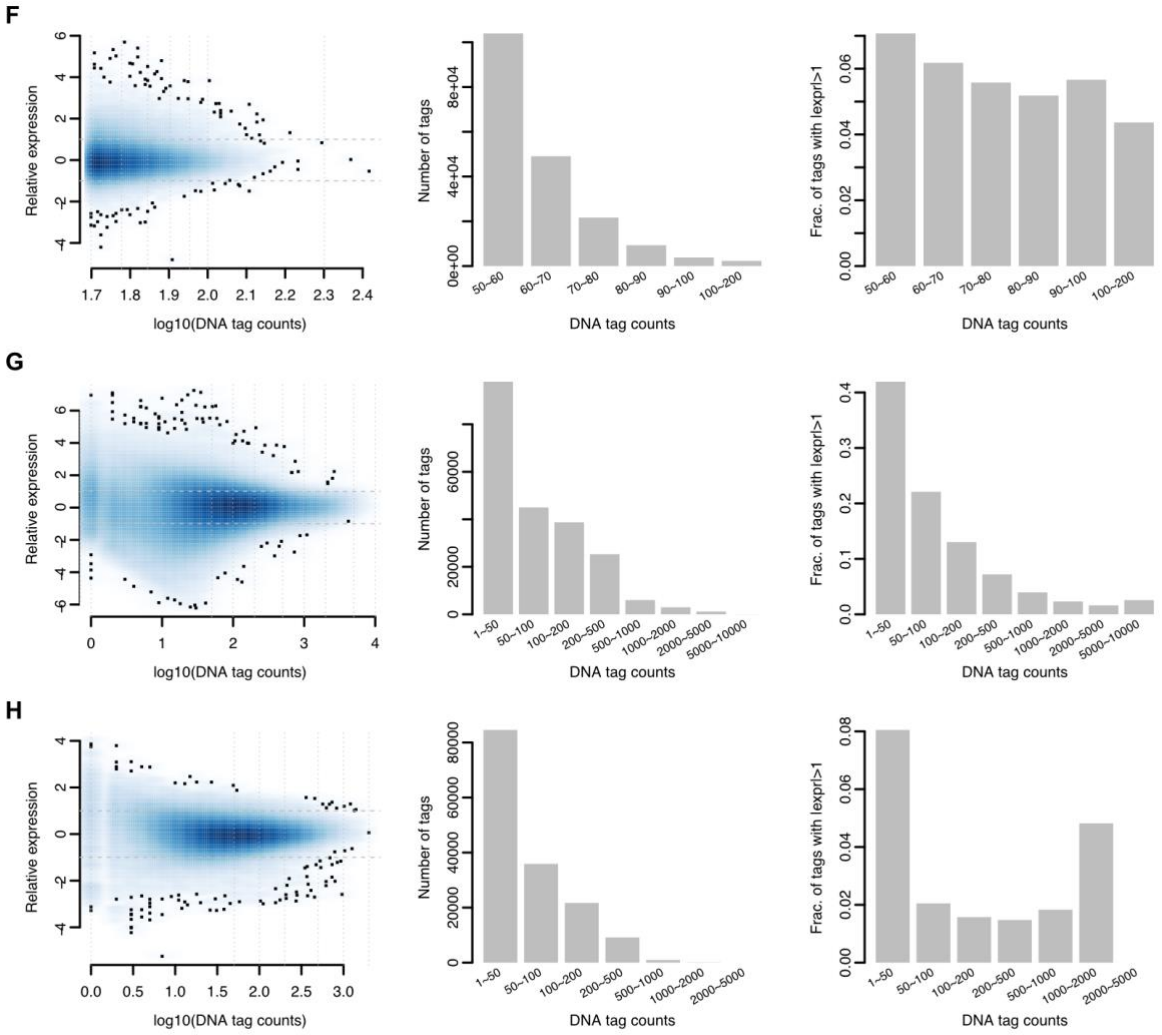

Supplemental Figure S1: DNA tags with low read counts are more variable. The relationships between DNA (plasmid) read counts and their relative expression **(1st column)**, tag frequencies binned by their DNA read counts **(2nd column)**, and tag fractions with at least two-fold relative expression binned by their DNA read counts **(3rd column)** from the Melnikov *et al.* 2012 **(A, Mel12)**, Kheradpour *et al.* 2013 for HepG2 **(B, Khe13)** and K562 **(C, Khe13K)**, Ernst *et al.* 2016 for HepG2 **(D, Ern16)** and K562 **(E, Ern16K)**, Tewhey *et al.* 2016 **(F, Tew16)**, Ulirsch *et al.* 2016 **(G, Uli16)**, and Inoue *et al.* 2017 **(H, Ino17)** studies.

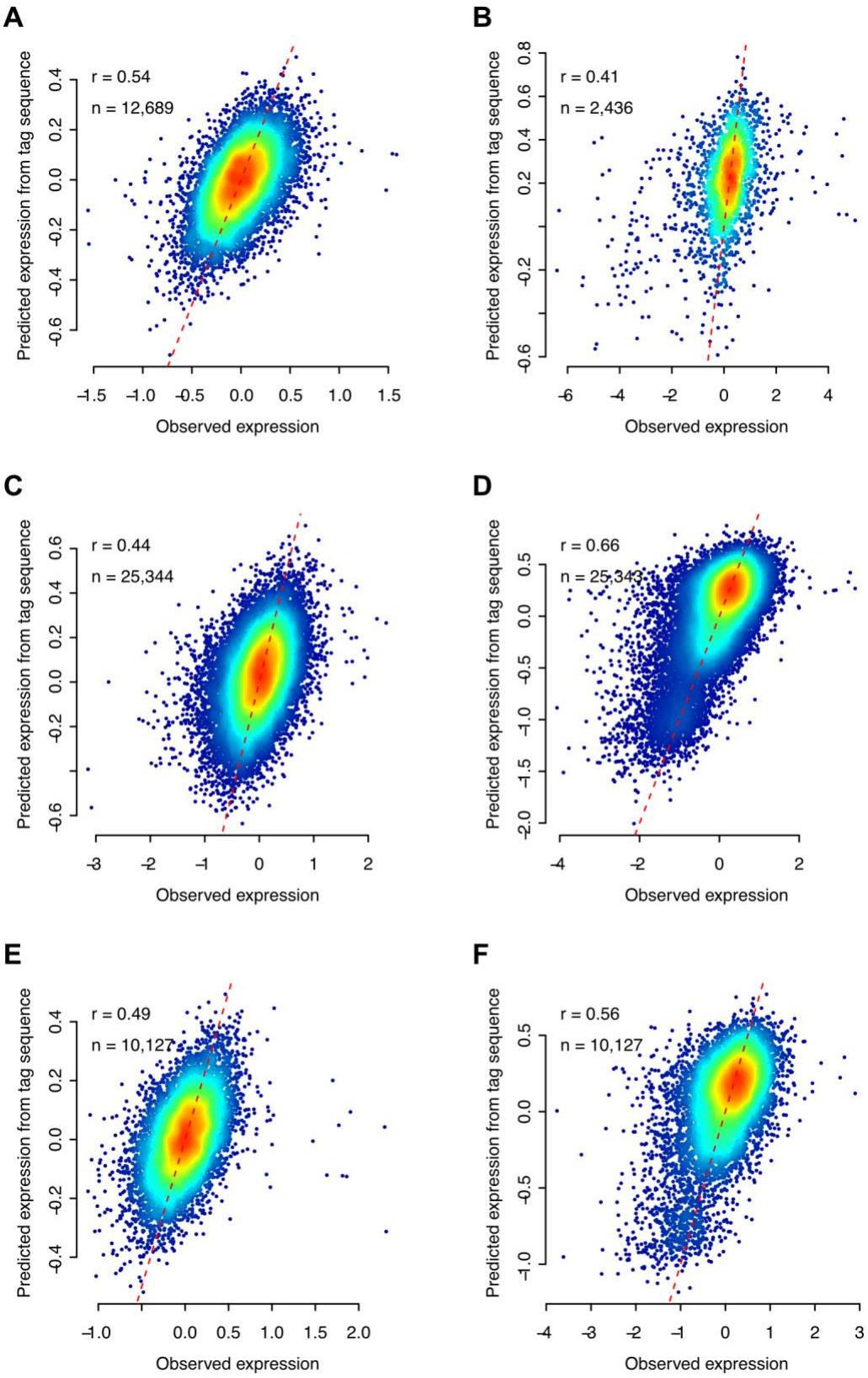

(Continue to the next page)

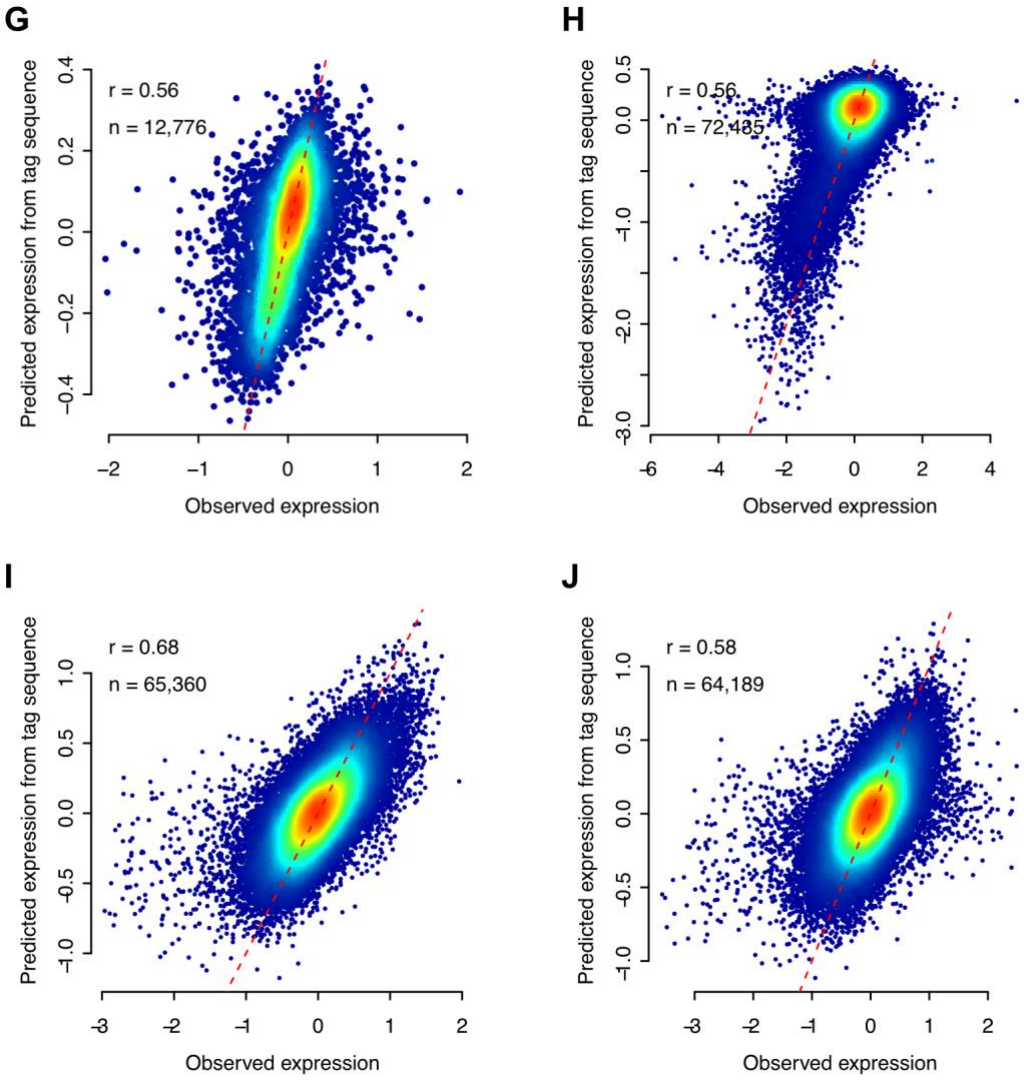

Supplemental Figure S2: Support vector regression accurately predicts tag sequence effects. The observed relative expression (X-axis) is compared to the predicted expression from tag sequence (Y-axis) using 5-fold cross-validation for the data in Melnikov *et al.* 2012 **(A, Mel12)**, Mogno *et al.* 2013 **(B, Mog13)** Kheradpour *et al.* 2013 for HepG2 **(C, Khe13)**, and K562 **(D, Khe13K)**, Ernst *et al.* 2016 for HepG2 **(E, Ern16)** and K562 **(F, Ern16K)**, Kwasnieski et al. 2014, **(G, Kwa14)** Tewhey *et al.* 2016 **(H, Tew16)** and Inoue *et al.* 2017 using episomal **(I, Ino17)** and integrated **(J, Ino17W)** constructs, respectively. Pearson correlations (*r*) and numbers of data points (*n*) are shown. Red dashed lines indicate the Y = X line. The density of data points is represented by a color heatmap calculated by a bivariate Gaussian Kernel Density Estimate function with default parameters (see: densCols() and bkde2D() functions in R for details).

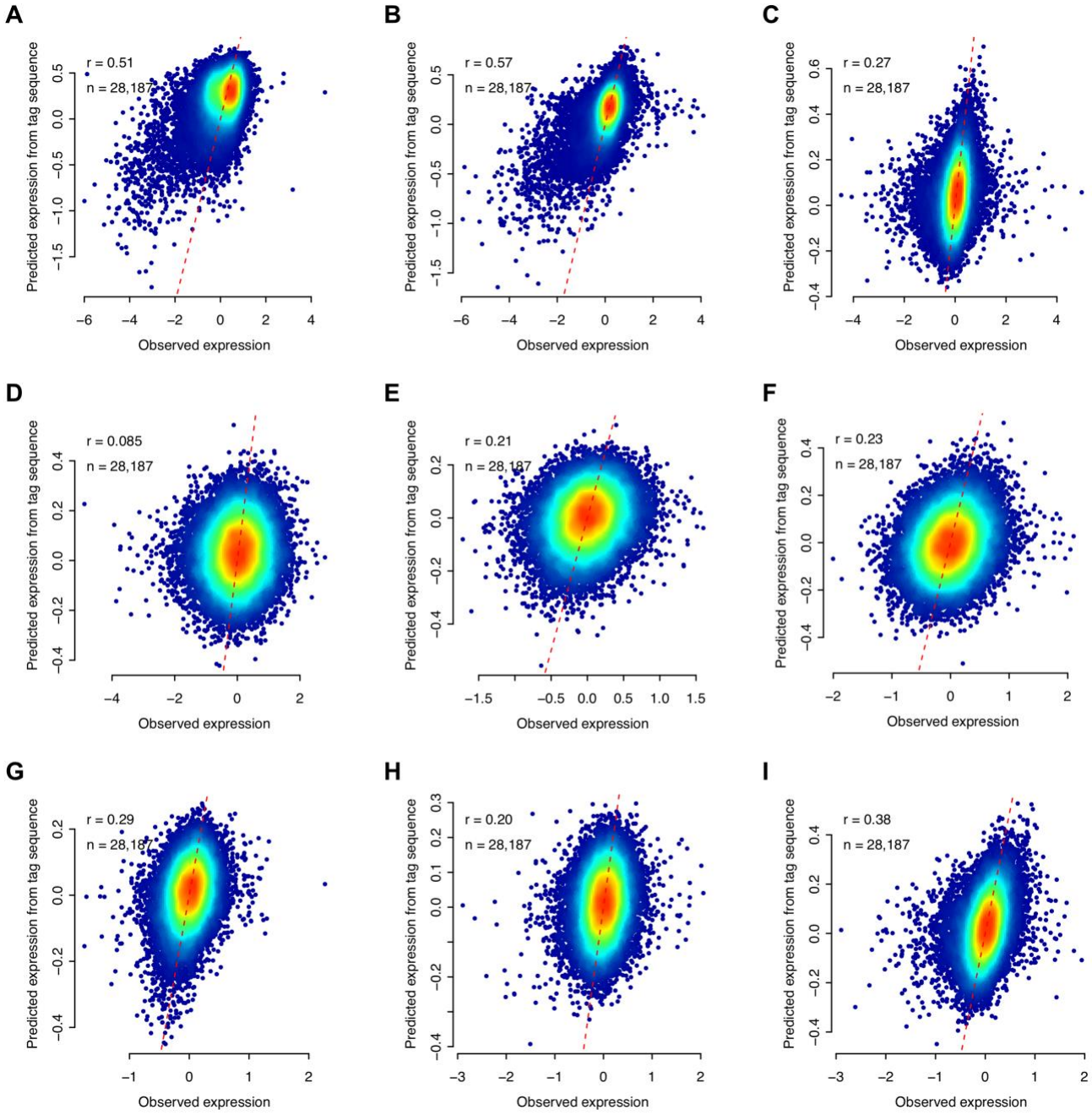

Supplemental Figure S3: MTSA analysis of the nine MPRA data sets from Klein et al. 2020. Observed relative expression are compared to MTSA predicted expression from 5-fold cross-validation for the original STARR-seq **(A, HSS)**; STARR-seq with no minimal promoter **(B, ORI)**; pGL4.23c vector **(C, pGL4)**; lentiMPRAs with both the enhancer library and barcodes in the 3' UTR of the reporter packaged with MT integrase **(D, 3'/3' MT)** and WT integrase **(E, 3'/3' WT)**; lentiMPRAs with the enhancer library upstream of the minimal promoter and the associated barcodes in the 3′ UTR of the reporter gene with MT integrase **(F, 5'/3' MT)** and WT integrase **(G, 5'/3' WT)**; lentiMPRAs with the enhancer library upstream of the minimal promoter and barcodes in the 5' UTR of the reporter with MT integrase **(H, 5'/5' MT)** and WT integrase **(I, 5'/5' WT)**.

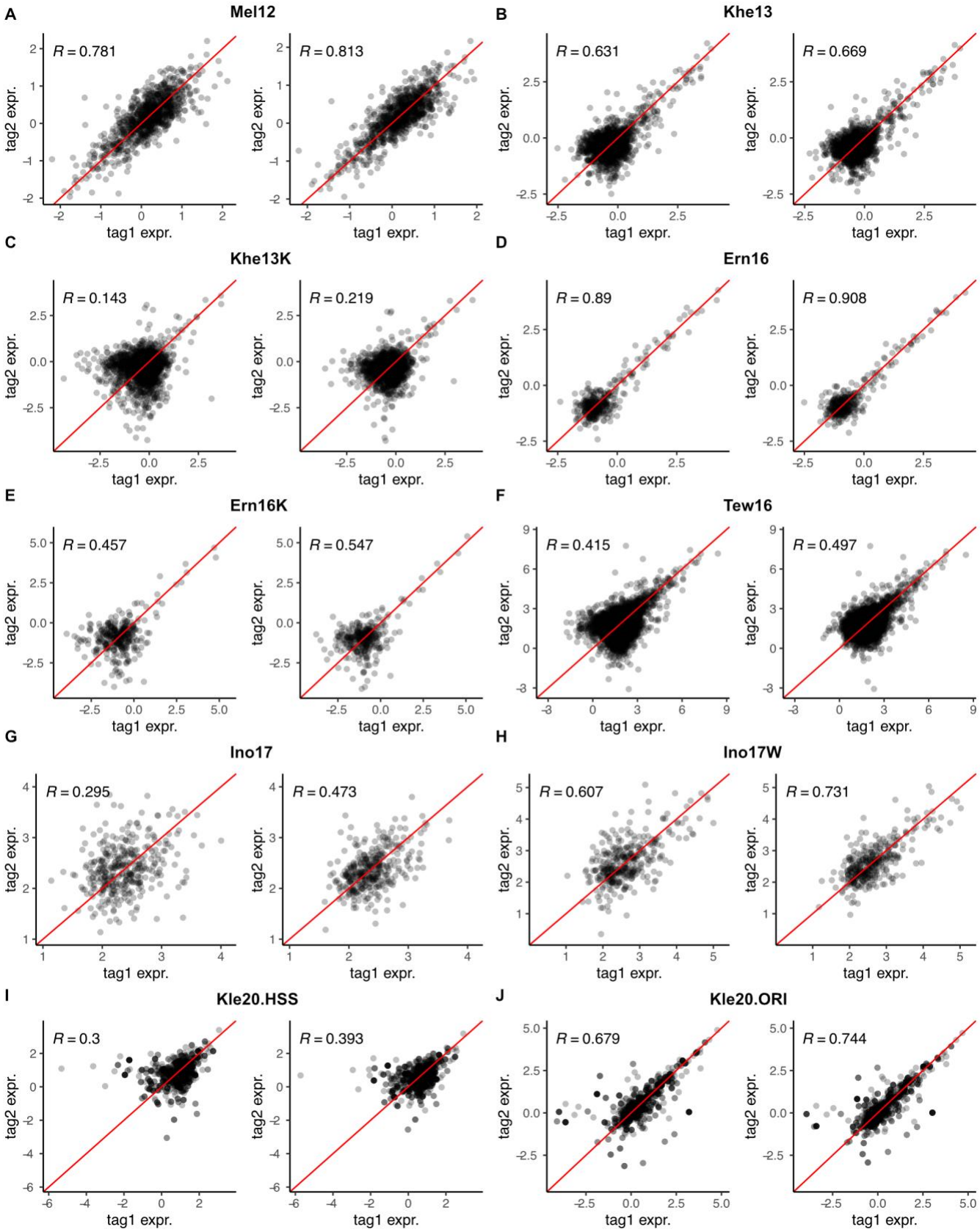

(Continue to the next page)

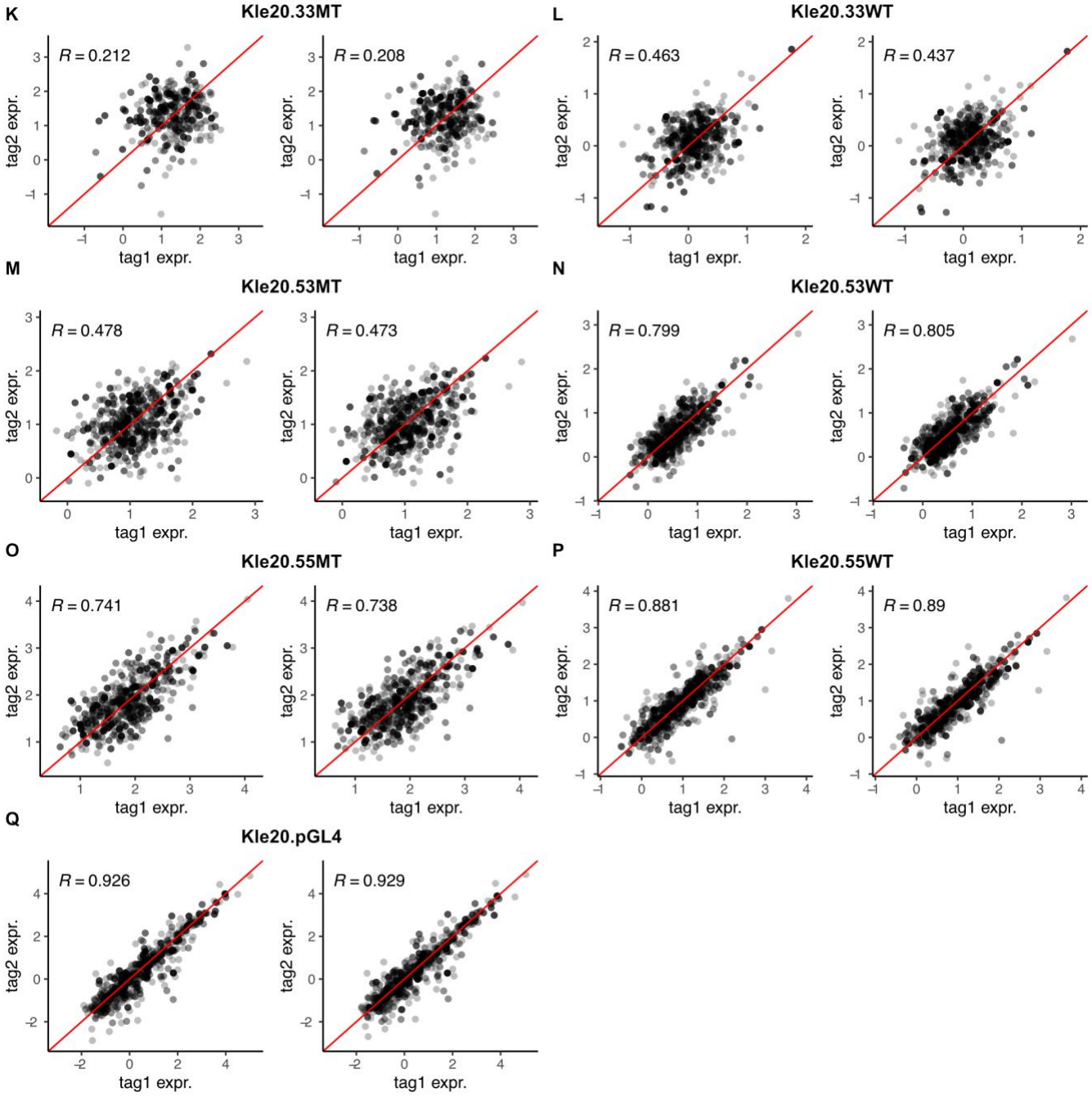

Supplemental Figure S4: Tag sequence-based correction reduces variation within CREs. Scatter plots of tag expression of two randomly selected tags within CREs are shown with (*right*) and without (*left*) MTSA correction in a $\log_2$ scale, for the data in Mel12 **(A)**, Khe13 **(B)** and Khe13K **(C)**, Ern16 **(D),** Ern16K **(E)**, Tew16 **(F),** Ino17 **(G),** Ino17W **(H)**, Kle20.HSS **(I)**, Kle20.ORI **(J)**, Kle20.33MT **(K)**, Kle20.33WT **(L)**, Kle20.53MT **(M)**, Kle20.53WT **(N)**, Kle20.55MT **(O)**, Kle20.55WT **(P)**, and Kle20.pGL4 **(Q)** respectively. *R* is the Pearson correlation coefficient, and the red dashed line indicates the Y = X line.

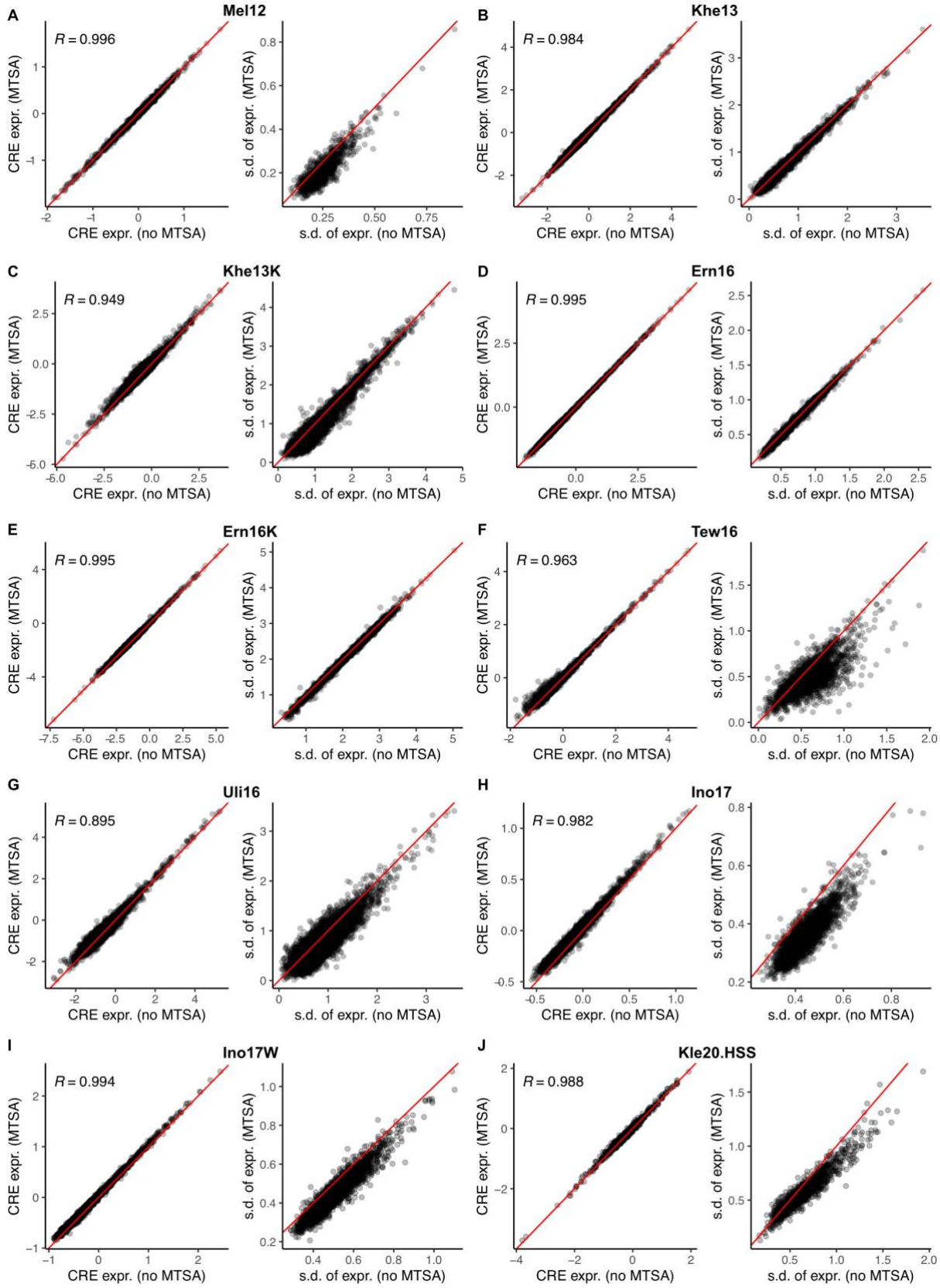

(Continue to the next page)

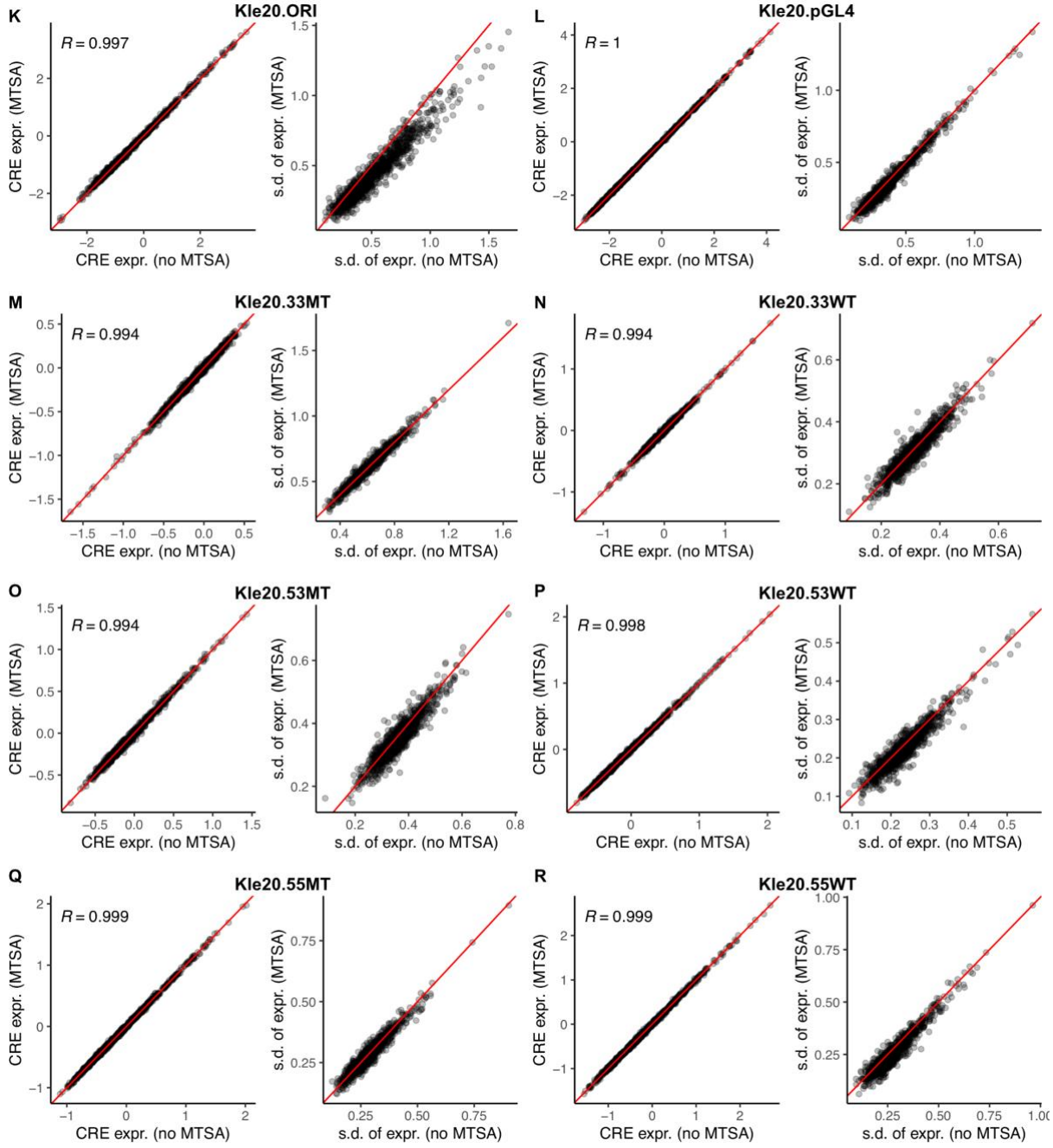

Supplemental Figure S5: MTSA correction marginally affects CRE expression but significantly reduces its variance across tags. The correlation between CRE-level expression with and without MTSA correction **(the 1st and 3rd column)** and their standard deviation **(the 2nd and 4th column)** are shown for the data in Mel12 **(A)**, Khe13 **(B)**, Khe13K **(C)**, Ern16 **(D)**, Ern16K **(E)**, Tew16 **(F),** Uli16 **(G)**, Ino17 **(H)**, Ino17W **(I)**, Kle20.HSS **(J)**, Kle20.ORI **(K)**, Kle20.pGL4 **(L)**, Kle20.33MT **(M)**, Kle20.33WT **(N)**, Kle20.53MT **(O)**, Kle20.53WT **(P)**, Kle20.55MT **(Q)**, Kle20.55WT **(R)**. *R* is the Spearman's correlation, and the red line indicates the Y = X line. The average of $\log_2$(RNA/DNA) across tags is the CRE-level expression. We only used CREs with at least 3 tags and tags with at least one read per million.

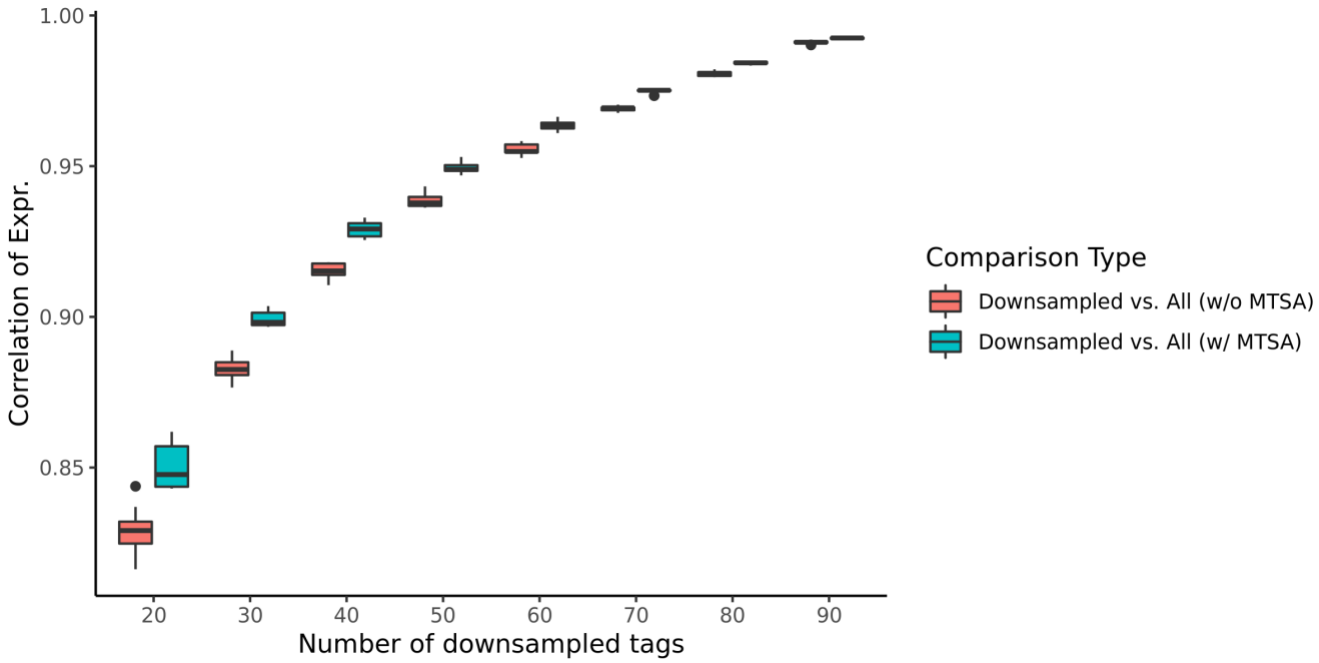

Supplemental Figure S6: Correlation of expression between down-sampled tags and all tags before and after MTSA correction. For each of the down-sampled tags with n=20, 30, ..., 90, we calculated CRE-level expression and compared them to those calculated using all tags (n=100) with and without MTSA correction. MTSA correction was applied to both. For each tag number, we repeated 10 times and calculated average Spearman correlation coefficients. Improvement achieved by MTSA correction is gradually attenuated and the average improvement is <2% when n>50. The average of $\log_2$(RNA/DNA) across tags is the CRE-level expression. We only used CREs with at least three tags, and tags with at least one read per million.

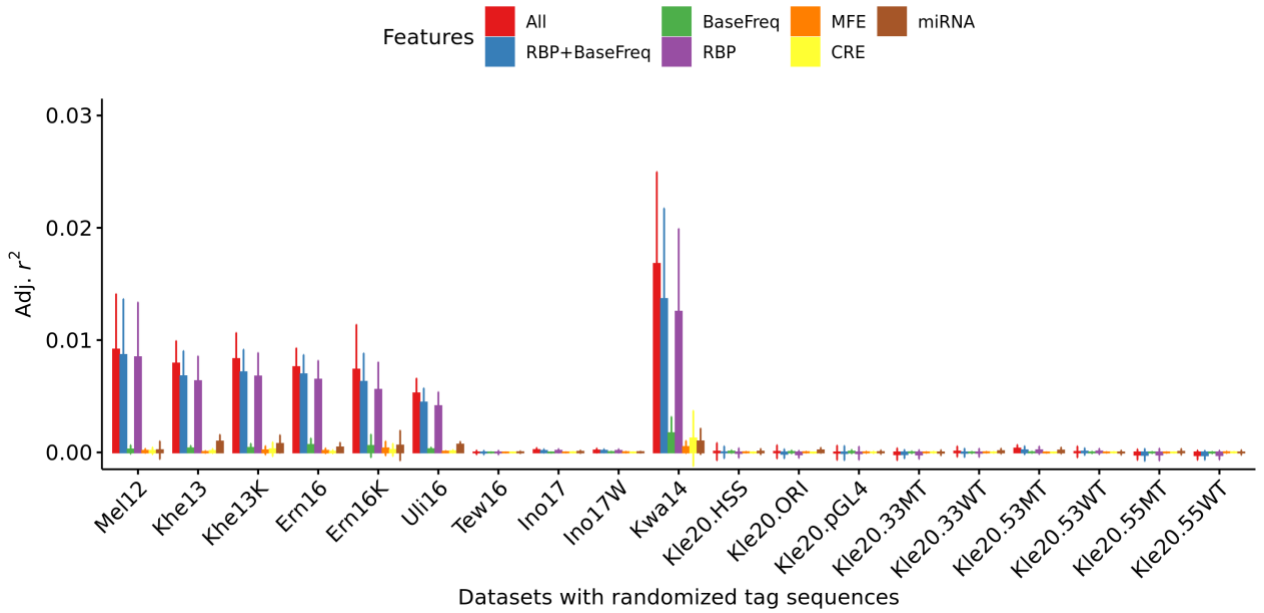

Supplemental Figure S7: Randomized tag sequences do not explain the variation of relative tag expression attributed to specific biological features. As a negative control, we randomized the tag sequences and performed the same multivariate linear regression analysis as **Fig. 5**. We repeated the analysis ten times to estimate the mean and the standard deviation of adjusted r^2. We found that <1% of the variance can be explained by the randomized tags for all data sets, except Kwa14.

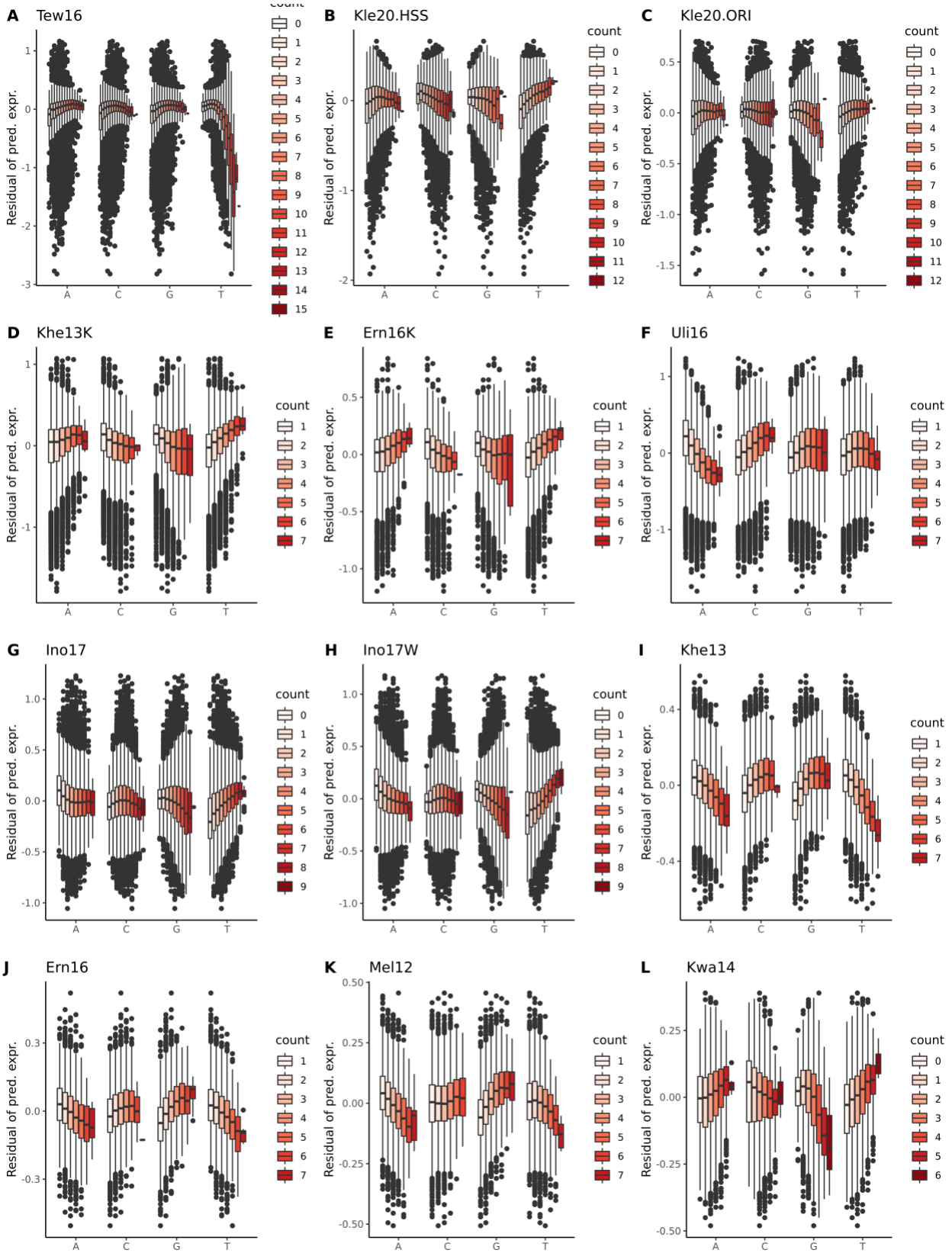

(Continue to the next page)

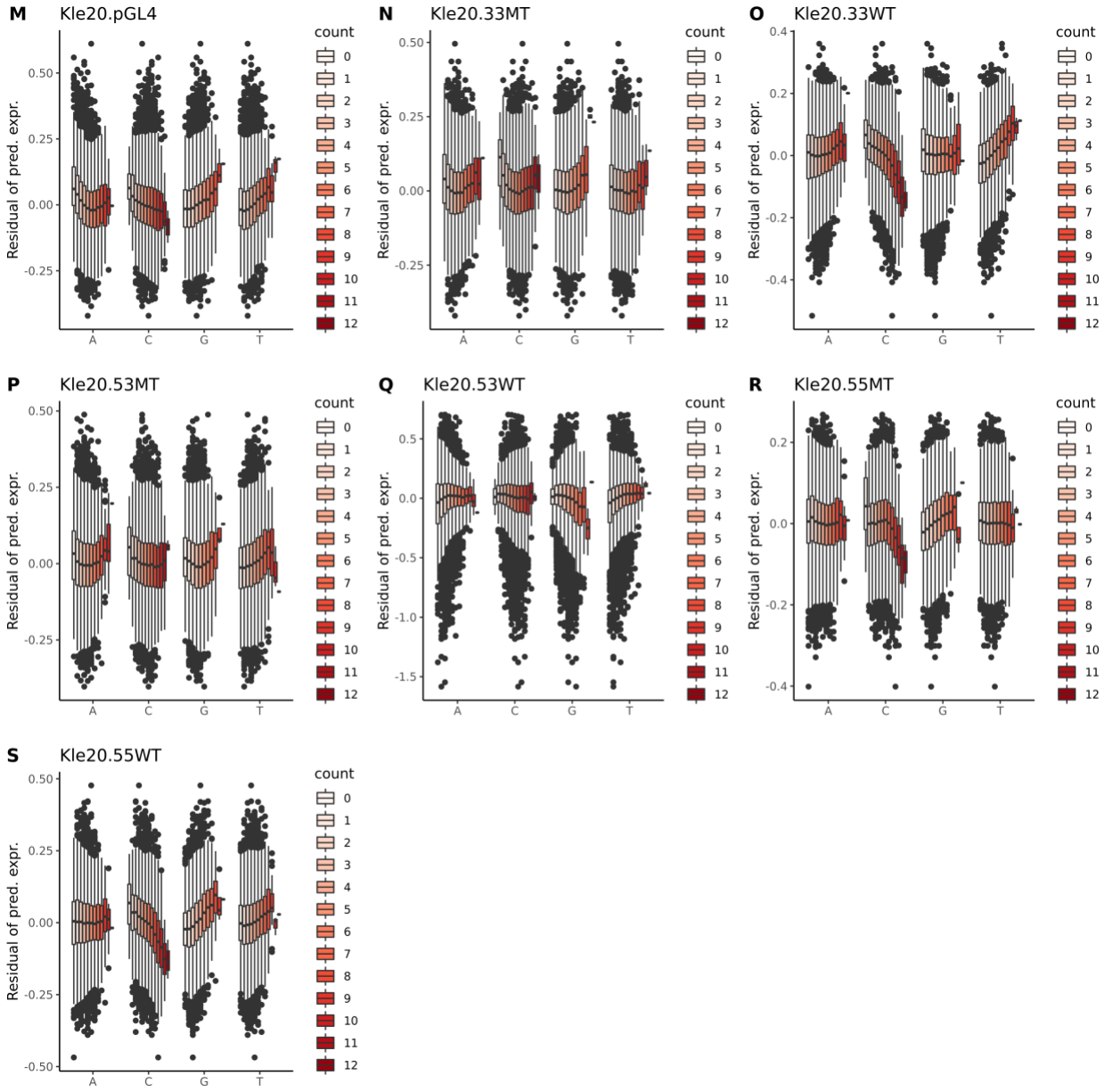

Supplemental Figure S8: Effect of base counts on relative expression is specific to experimental designs and cell types. Distributions of residuals of the predicted relative expression are stratified by base counts for Tew16 **(A)**, Kle20.HSS **(B)**, and Kle20.ORI **(C)**, Khe13K **(D)**, Ern16K **(E)**, Uli16 **(F)**, Ino17 **(G)**, Ino17W **(H)**, Khe13 **(I)**, Ern16 **(J)**, Mel12 **(K)**, Kwa14 **(L)**, Kle20.pGL4 **(M)**, Kle20.33MT **(N)**, Kle20.33WT **(O)**, Kle20.53MT **(P)**, Kle20.53WT **(Q)**, Kle20.55MT **(R)**, and Kle20.55WT **(S)**. In general, the count of T shows the strongest effect on the predicted expression, although the direction of effect is specific to the experiment and cell types. Data sets associated with long tags **(A, G,** and **H)**, with the STARR-seq construct **(B, C)**, or measured in K562 **(D, E,** and **F)** tend to have more extreme outliers than other data sets **(H-S)**.

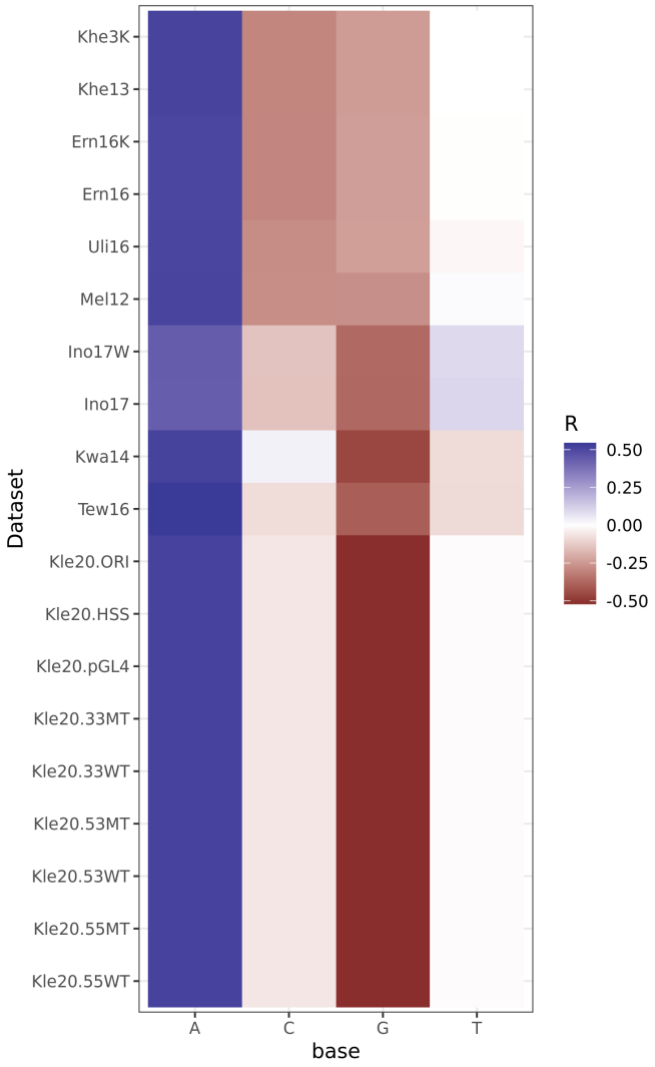

Supplemental Figure S9: Base counts in tags strongly correlate with minimum free energy of mRNA secondary structure. For each of the data sets, correlations of MFE and each of the base counts in tags are shown as a heatmap. Expectedly, MFE is strongly positively correlated with the count of 'A' for all data sets, while negatively correlated with 'C', and 'G' counts.

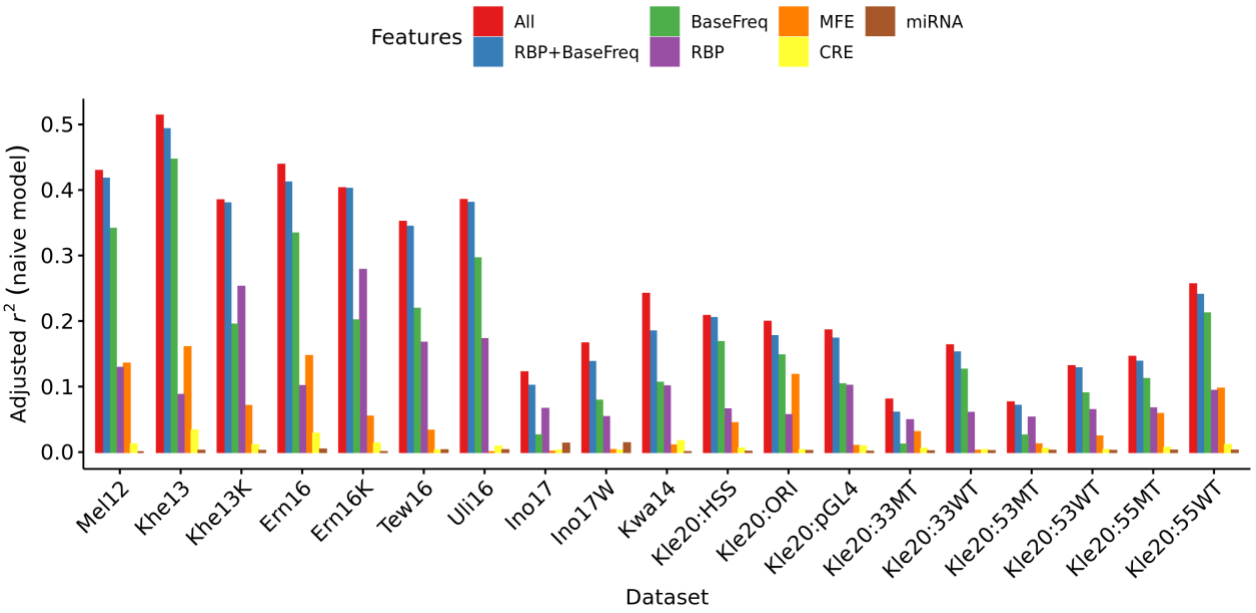

Supplemental Figure S10: Base counts capture signals that can be explained by other potential biological mechanisms. Multivariate linear regression analyses were performed similar to **Fig. 5**, except that the dependent variable (predicted relative expression) was not adjusted by other features sets. The BaseFreq feature set captures more variation in these naïve models than the residual models in **Fig. 5** because it captures variations explained by other biological features (i.e., MFE, RBP, and CRE). Similarly, MFE explains up to 15% of variation in expression if it is not adjusted by BaseFreq. **BaseFreq**: base frequencies in tag sequences, **MFE**: minimum free energy of mRNA secondary structures, **CRE**: tags as cis-regulatory elements, **miRNA**: microRNA binding sites, **RBP**: RNA binding protein binding sites, **RBP+BaseFreq**: RBP and BaseFreq features combined, **All**: all features combined.

Data set ID	Year	Cell Type	# of CREs	Tags per CRE	# of Constructs	Oligo Length	CRE Length	Tag Length	Restriction Sites	Reporter Gene	Transfection strategies
Mel12	2012	HEK293	1,000	13	13,000	142	87	10	KpnI – XbaI	Luciferase	Transient using lipofectamine
Khe13	2013	HepG2, K562	5,400	10	54,000	200	145	10	KpnI – XbaI	Luciferase	(1) HepG: Transient using Fugene HD (2) K562: Transient using electroporation (Nucleofector II)
Mog13	2013	Yeast (SC)	2,467	Var.	6,908	.	Var.	15	EagI – XbaI	YFP	Integrated at TRP1 locus
Kwa14	2014	K562	3,237	4	12,931	200	130	9	XhoI – SphI	DsRed	Transient using electroporation (Neon system)
Ern16	2016	HepG2, K562	2,250	24	54,000	200	145	10	KpnI – XbaI	Luciferase	Same as **Khe13**
Tew16	2016	LCLs	7,500	Var.	~3.4M	180	150	20	.	GFP	Transient using electroporation (Neon system)
Uli16	2016	K562	16,534	14	231,476	200	145	10	KpnI – XbaI	Luciferase	K562: Transient using electroporation (Nucleofector II)
Ino17	2017	HepG2	2,440	100	244,000	230	171	15	SbfI – EcoRI	EGFP	Transient/Integrated using lentivirus (jetPRIME)
Kle20	2020	HepG2	2,440	Var.	4.1M ~ 9.8M	230	171	15	SbfI – EcoRI	GFP	(1) HSS,ORI,pGL4: transient using X-tremeGENE HP (2) 5/5WT,5/3WT,3/3WT: integrated using lentivirus (3) 5/5MT,5/3MT,3/3MT: transient using lentivirus

Supplemental Table S1: Design details of the public MPRA data sets evaluated in this study. Details of nine different MPRA studies are summarized. Studies that used variable number of tags per CRE are marked as "Var." SC: Saccharomyces cerevisiae; YFP: yellow fluorescent protein; DsRed: red fluorescent protein; EGFP: enhanced green fluorescent protein; LCLs; lymphoblastoid cell lines.

Data set ID	Correlation after 1st training	Correlation after 2nd training	Difference in Correlation
Mel12	0.50	0.54	+0.04
Mog13	0.39	0.41	+0.02
Khe13	0.38	0.44	+0.06
Khe13K	0.59	0.66	+0.07
Kwa14	0.44	0.56	+0.12
Ern16	0.44	0.49	+0.05
Ern16K	0.51	0.56	+0.05
Tew16	0.54	0.56	+0.02
Tew16N	0.28	0.30	+0.02
Uli16	0.65	0.71	+0.06
Ino17	0.66	0.68	+0.02
Ino17W	0.57	0.58	+0.01
Kle20.HSS	0.50	0.51	+0.01
Kle20.ORI	0.56	0.57	+0.01
Kle20.pGL4	0.26	0.27	+0.01
Kle20.33MT	0.073	0.085	+0.01
Kle20.33WT	0.20	0.21	+0.01
Kle20.53MT	0.22	0.23	+0.01
Kle20.53WT	0.27	0.29	+0.02
Kle20.55MT	0.18	0.20	+0.02
Kle20.55WT	0.36	0.38	+0.02

Supplemental Table S2: Model performance is consistently improved by bias correction based on the initial training. For each of the data sets, we calculated correlations between the observed relative expression and the predicted expression after the first training (2nd column) as well as the second training (3rd column). The correlation values in the 3rd column are the same as the *r* values shown in **Fig. 2A**, **Supplemental Fig. S2**, and **Supplemental Fig. S3**. Differences in the correlations are shown in the 4th column.

Data set ID	Correlation using reverse complement sequences as the same features	Correlation using reverse complement sequences as distinct features	Difference in Correlation
Mel12	0.53	0.54	+0.01
Mog13	0.22	0.41	+0.19
Khe13	0.43	0.44	+0.01
Khe 13K	0.65	0.66	+0.01
Kwa14	0.55	0.56	+0.01
Ern16	0.48	0.49	+0.01
Ern16K	0.55	0.56	+0.01
Tew16	0.42	0.56	+0.14
Tew16N	0.22	0.30	+0.08
Uli16	0.70	0.71	+0.01
Ino17	0.64	0.68	+0.04
Ino17W	0.55	0.58	+0.03
Kle20.HSS	0.49	0.51	+0.02
Kle20.ORI	0.54	0.57	+0.03
Kle20.pGL4	0.27	0.27	0
Kle20.33MT	0.080	0.085	0.005
Kle20.33WT	0.21	0.21	0
Kle20.53MT	0.22	0.23	+0.01
Kle20.53WT	0.28	0.29	+0.01
Kle20.55MT	0.20	0.20	0
Kle20.55WT	0.35	0.38	+0.03

Supplemental Table S3: Using reverse complement sequences as distinct features marginally but consistently improves model performance. MTSA models were retrained by treating the reverse complement gapped k-mer pairs as the same features, with an assumption that DNA sequences, rather than mRNA sequences, play a major role in affecting the tag expression. The correlation between the observed relative expression and the predicted expression by these models are shown in the 2nd column. The correlation values in the 3rd column are the same as the *r* values shown in **Fig. 2A**, **Supplemental Fig. S2**, and **Supplemental Fig. S3**. Differences in the correlations are shown in the 4th column.

Data set ID	Correlation of CREs between replicates before MTSA correction	Correlation of CREs between replicates after MTSA correction	Difference in Correlation
Mel12	0.78	0.78	0
Khe13	0.73	0.72	-0.01
Khe 13K	0.45	0.44	-0.01
Ern16	0.92	0.92	0
Ern16K	0.70	0.70	0
Uli16	0.58	0.58	0
Tew16	0.92	0.92	0
Ino17	0.98	0.97	-0.01
Ino17W	0.99	0.99	0
Kle20.HSS	0.93	0.93	0
Kle20.ORI	0.99	0.99	0
Kle20.pGL4	0.99	0.99	0
Kle20.33MT	0.55	0.55	0
Kle20.33WT	0.86	0.86	0
Kle20.53MT	0.89	0.89	0
Kle20.53WT	0.95	0.95	0
Kle20.55MT	0.96	0.96	0
Kle20.55WT	0.95	0.95	0

Supplemental Table S4: MTSA correction does not improve the correlation of CRE level expression between experimental replicates. Correlation of CRE-level expression between replicates before and after MTSA correction are shown for the eight different MPRA data sets. The average of $\log_2$(RNA/DNA) across tags was used as the CRE-level expression. We only considered CREs with at least three tags, and tags with at least one read counts per million.

Mel12			Khe13			Khe13K		
8-mer	**SVRW**	**RBP**	**8-mer**	**SVRW**	**RBP**	**8-mer**	**SVRW**	**RBP**
TCGAGATC	-0.34	M348_0.6	ATATATAA	-0.42	M055_0.6	TCGAGATC	-2.17	M348_0.6
AAATATAT	-0.33	.	ATAAATAA	-0.42	.	ACGAGATC	-1.82	M348_0.6
CCACGAGA	-0.32	.	TAGATATA	-0.4	.	CCGAGATC	-1.79	.
AAATAAAT	-0.31	M176_0.6	TATATATA	-0.4	M055_0.6	GCGAGATC	-1.78	.
CTAGAAAA	-0.3	.	AAAAATTA	-0.38	.	CTCGAGAT	-1.22	M348_0.6
GAAGATTC	-0.3	.	ATAAATTA	-0.37	.	CCCGAGAT	-1.21	.
AAATAATT	-0.3	.	TATAAATA	-0.37	.	CGCGAGAT	-1.17	.
AAAAATAT	-0.3	.	AATAATTA	-0.37	M001_0.6	CACGAGAT	-1.16	M348_0.6
ATATATAT	-0.29	M055_0.6	AAAAATAA	-0.37	.	TTCGAGAT	-1.15	M348_0.6
ATATAAAT	-0.29	.	ATAGATAA	-0.36	M210_0.6	CCTCGAGA	-1.14	.
AGATGAGA	0.21	.	GAGAGGCC	0.32	.	GAGATCAA	0.63	.
AGTGGCCT	0.21	.	AAAAGGCC	0.32	.	GAAAGATC	0.63	M250_0.6
AGAGGTCC	0.22	.	AAAATGGC	0.33	.	TAAAGATC	0.7	M250_0.6
AGTGAGAA	0.22	.	AGAGGCCC	0.35	.	AAAAGATC	0.7	M148_0.6
CTAGAGCT	0.23	.	AGAGGCCT	0.35	.	CGAGATCA	0.7	.
AGAGGCCG	0.23	.	AGAAGCCG	0.35	.	AGAGATCA	0.71	.
CTAGAGGC	0.24	.	AGAGGCCG	0.36	.	AGAGATCT	0.72	.
TAGAGGCC	0.26	.	**CTAGA**GGC	0.4	.	GGAAGATC	0.74	M250_0.6
AGAGGCCT	0.26	.	TAGAGGCC	0.41	.	AGAGATCC	0.78	.
CTAGAGCC	0.34	.	**CTAGA**GCC	0.42	.	AGAGATCG	0.79	.
Ern16			**Ern16K**			**Tew16**		
8-mer	**SVRW**	**RBP**	**8-mer**	**SVRW**	**RBP**	**8-mer**	**SVRW**	**RBP**
ATATATAT	-0.35	M055_0.6	TCGAGATC	-1.61	M348_0.6	TTTTTTTT	-2.54	M012_0.6
TATATATA	-0.35	M055_0.6	ACGAGATC	-1.43	M348_0.6	ATTTTTTT	-2.42	M012_0.6
ATATATAA	-0.34	M055_0.6	GCGAGATC	-1.4	.	TTTTTTTA	-2.27	M012_0.6
AAATATAT	-0.33	.	CCGAGATC	-1.31	.	AATTTTTT	-2.15	M025_0.6
ATATATTT	-0.32	.	GTCGAGAT	-0.94	M348_0.6	TATTTTTT	-2.09	M012_0.6
ATAAATAA	-0.32	.	TCGAGAGC	-0.87	.	CTTTTTTT	-2.09	M012_0.6
AGATATAT	-0.31	M233_0.6	TTCGAGAT	-0.87	M348_0.6	TTTTTTTG	-2.05	M012_0.6
ATATATAG	-0.3	M055_0.6	ACGAGAGC	-0.85	.	ACTTTTTT	-1.98	M012_0.6
AATATATT	-0.3	.	GGCGAGAT	-0.8	.	TCTTTTTT	-1.93	M012_0.6
ATATATTA	-0.3	.	CCCGAGAT	-0.79	.	TTTTTTAT	-1.82	M075_0.6
AGCCGGAA	0.22	M290_0.6	CAAAGATC	0.44	M250_0.6	AGGGGCGG	0.25	.
AAAAGGCC	0.23	.	GGAAAGAT	0.44	.	CTAAAATG	0.25	M060_0.6
AGAAGCCG	0.23	.	GGGAAGAT	0.45	.	AAGGGCGG	0.25	.
AGAGCCCG	0.25	.	GAGAAGAT	0.45	M148_0.6	GACGGTGC	0.25	.
AGAGGCCC	0.25	.	TATAGATC	0.48	.	ATTTGGAA	0.25	M290_0.6
AGAGGCCT	0.29	.	AGAGATCC	0.49	.	GGGCGGGC	0.26	M151_0.6
AGAGGCCG	0.29	.	GGAAGATC	0.52	M250_0.6	TGGGCGGA	0.28	M065_0.6
TAGAGGCC	0.33	.	TAAAGATC	0.56	M250_0.6	GGGCGGTT	0.28	.
CTAGAGCC	0.33	.	AAAAGATC	0.56	M148_0.6	ATGGGCGG	0.28	.
CTAGAGGC	0.34	.	GAAAGATC	0.6	M250_0.6	GGGCGGAC	0.31	M065_0.6
Uli16			**Kwa14**			**Ino17**		
8-mer	**SVRW**	**RBP**	**8-mer**	**SVRW**	**RBP**	**8-mer**	**SVRW**	**RBP**
TCGAGATC	-1.63	M348_0.6	**ATGCC**GCC	-0.42	.	CCCTCGAC	-0.81	.
GCGAGATC	-1.55	.	**ATGCC**GTC	-0.36	.	TCCCTCGA	-0.77	.
ACGAGATC	-1.49	M348_0.6	**ATGCC**GCA	-0.35	.	CCTCGACG	-0.77	.
CCGAGATC	-1.3	.	**ATGCC**GAG	-0.35	.	TTCCCTCG	-0.74	.
TAGAGATC	-1.05	.	**ATGCC**GCT	-0.35	.	GTCCCTCG	-0.65	.
GAGAGATC	-1.02	M147_0.6	**ATGCC**GGA	-0.34	.	TAAGGCAT	-0.6	.
AAGAGATC	-1.01	.	**ATGCC**GAT	-0.34	.	GCAGCAGC	-0.6	.
ATCGAGAT	-0.94	M348_0.6	**ATGCC**GGG	-0.32	.	CCCTCGGC	-0.59	.
ACCGAGAT	-0.93	.	TGCCGCCA	-0.32	.	AGGCATTA	-0.57	.
GGCGAGAT	-0.9	.	**ATGCC**GGC	-0.31	.	TCGAGGCA	-0.57	.
CGTGATCG	0.86	.	GCCATGTG	0.22	.	CGGAACCT	0.66	.
CGAGATGG	0.86	.	CC**ATGCC**G	0.22	.	ACCGGAAC	0.66	M291_0.6
CGTGATCA	0.89	.	**ATGCC**ATA	0.22	.	GAACCGGA	0.69	.
CGTCAGAT	0.93	.	**ATGCC**AAG	0.23	.	CCGGACCC	0.72	.
CGCGATCA	0.94	.	TGCCATGC	0.23	.	GGAACCCT	0.72	.
CGAGATCT	0.94	.	**ATGCC**ACG	0.23	.	TCGGAACC	0.76	.
AGAGATCG	1	.	GCCACGTG	0.24	.	CCGGAGCC	0.79	.
CGAGATCC	1.01	.	**ATGCC**AGT	0.25	.	GGAACCCA	0.81	.
CGAGATCA	1.08	.	**ATGCC**ATT	0.25	.	CCGGAACC	0.92	M291_0.6
CGAGATCG	1.11	.	**ATGCC**ATG	0.32	.	CGGAACCC	0.98	.

(Continue to the next page)

Kle20.HSS			Kle20.ORI			Kle20.pGL4		
8-mer	**SVRW**	**RBP**	**8-mer**	**SVRW**	**RBP**	**8-mer**	**SVRW**	**RBP**
GGCCGGCC	-1.68	.	GGCCGGCC	-1.54	.	ATCACGTG	-0.15	.
CGGCCGGC	-1.39	.	GCCGGCCG	-1.38	.	CACGTGCA	-0.15	.
GCCGGCCG	-1.37	.	CGGCCGGC	-1.23	.	TAAGACGT	-0.14	.
GCCGGCCC	-1.24	.	AGCCGGCC	-1.19	.	AAGGACCA	-0.14	M072_0.6
GCCGGCCA	-1.2	.	GCCGGCCC	-1.14	.	**CTAAG**ACG	-0.14	.
AGCCGGCC	-1.2	.	GCCGGCCA	-1.09	.	ATGCATCC	-0.13	.
GGCCGACC	-1.15	.	GCGGCCGG	-1.03	.	ACCGTGCA	-0.13	.
CGGCCGAC	-1.01	.	CCGGCCGG	-0.98	.	CACGTGTC	-0.13	.
GCGGCCGG	-1.01	.	CGCCGGCC	-0.97	.	ACCACGTG	-0.13	.
CCGGCCGG	-1	.	GGCCGACC	-0.95	.	ATGCATTG	-0.13	.
CGGGTCAC	0.56	.	CGCAATTG	0.45	.	GGCCGCCA	0.34	M044_0.6
GGTCACGC	0.56	.	CCTCCATT	0.46	.	GCAGCCAT	0.35	.
CCTCCGGG	0.56	.	GTCGCCAT	0.46	.	TCCGCCAT	0.38	.
TTGTTCAC	0.56	.	GCCGCCAT	0.48	.	GTCGCCAT	0.38	.
GTTCCTCC	0.57	.	ACGCCATT	0.49	.	GGCGGCCA	0.38	.
CGGGACAC	0.57	.	CGCCATTA	0.51	.	CGGCCATT	0.44	.
GGGGTCAC	0.57	.	GACGCCAT	0.52	.	GCGGCCAT	0.45	.
GGGTCACA	0.59	.	TCCGCCAT	0.58	.	GCCGCCAT	0.51	.
TGGGTCAC	0.6	.	CCGCCATT	0.68	.	CGCCATTG	0.51	.
GGGTCACC	0.6	.	CGCCATTG	0.7	.	CCGCCATT	0.54	.
Kle20.33MT			**Kle20.33WT**			**Kle20.53MT**		
8-mer	**SVRW**	**RBP**	**8-mer**	**SVRW**	**RBP**	**8-mer**	**SVRW**	**RBP**
AGCGCCGT	-0.29	M050_0.6	CCCCCCCC	-0.50	M043_0.6	CACATTGC	-0.28	.
CGCCAGCA	-0.25	.	CCCCCCCT	-0.30	M043_0.6	**CTAAG**GTA	-0.26	.
CTAAGCGC	-0.22	.	CCCCCCCA	-0.29	M043_0.6	CACATCGC	-0.26	.
ACGGTCAT	-0.21	.	GCCCCCCC	-0.28	M043_0.6	CACATTCT	-0.25	.
CGCCAGTA	-0.21	.	ACCCCCCC	-0.28	M043_0.6	GGTAAGCC	-0.24	.
AGCGCCAT	-0.21	.	CCCCGCCC	-0.27	M044_0.6	CACATTGT	-0.23	.
CCAGCGCC	-0.21	M083_0.6	CCCCTCCC	-0.25	M043_0.6	TAAGGTAA	-0.23	.
AGTGTCAT	-0.21	.	CACCCCCC	-0.24	.	CACATTGG	-0.23	.
CAGCGCCG	-0.21	.	CCACCCCC	-0.23	.	CAGCGGCG	-0.22	.
CTATGCGC	-0.21	.	CCCCCACC	-0.23	.	TACATGCA	-0.21	.
GCCTCGAC	0.31	.	ACAGTTTC	0.19	.	TGTGTTCC	0.29	.
CCTCGACG	0.31	.	GCCCATGG	0.19	.	GCGATGTG	0.29	.
TCCCTCTC	0.31	.	TGTGGATC	0.19	.	ACACATTG	0.30	M008_0.6
GCCCTCGA	0.32	.	CTCAGCGG	0.19	.	TCACAGTG	0.31	.
CCTCGACT	0.32	.	GCGGCCGC	0.19	.	**CTAAG**CGA	0.32	.
CCCTCGAG	0.32	.	TCGGGGCT	0.20	.	AGCGATGT	0.32	.
AGGACTAT	0.32	M333_0.6	GCGGACGC	0.20	.	TCAAATTG	0.32	M236_0.6
CCTCGACA	0.33	.	**CTAAG**CGC	0.22	.	TTCACATT	0.39	.
GCCCCTCG	0.35	.	**CTAAG**CGT	0.22	.	CCACATTG	0.39	.
CCCTCGAC	0.39	.	**CTAAG**CGG	0.24	.	TCACATTG	0.52	.
Kle20.53WT			**Kle20.55MT**			**Kle20.55WT**		
8-mer	**SVRW**	**RBP**	**8-mer**	**SVRW**	**RBP**	**8-mer**	**SVRW**	**RBP**
AAGGTCCC	-0.40	.	CCTCGCCC	-0.36	.	CCTCGCCC	-0.33	.
AGGGTCCC	-0.36	.	CCCCGCCC	-0.31	M044_0.6	CCCCCCCC	-0.32	M043_0.6
AGGTCCCT	-0.34	.	CCCCCCCC	-0.26	M043_0.6	CCCCGCCC	-0.32	M044_0.6
TAAGGTCC	-0.32	.	CCCTCGCC	-0.23	.	CCCCCCCT	-0.23	M043_0.6
GGTCCCTC	-0.30	.	CCCCCGCC	-0.21	M044_0.6	CTCGCCCT	-0.20	.
AGGTCCCC	-0.29	.	CTCGCCCT	-0.21	.	CCCCCCTC	-0.19	.
TAGGTCCC	-0.29	.	AATGCATC	-0.20	.	CCACGCCC	-0.18	.
AAGGGTCC	-0.29	.	CCCCCCCT	-0.20	M043_0.6	CCCCTCCC	-0.17	M043_0.6
AGGGTCCT	-0.28	.	CGCCGCCC	-0.20	.	CTCCCCCC	-0.16	.
AAGGCCCC	-0.27	.	CCTTGCCC	-0.20	M177_0.6	ACATAAAC	-0.16	.
CGCCATTG	0.17	.	CTCAGCGC	0.18	M083_0.6	GTGTTCAC	0.37	.
G**CTAAG**AC	0.17	.	CAGGCGAC	0.18	.	GCTGTGTG	0.37	M049_0.6
CATCCTGC	0.17	.	GCTGCGAC	0.18	.	**CTAAG**CGT	0.37	.
TGGCGGCC	0.17	.	GATACAGC	0.18	.	TCACATTG	0.40	.
GGCGGCCC	0.17	.	AAGCCGGG	0.18	.	**CTAAG**CGC	0.40	.
AGCTCATC	0.18	.	AGAAATTT	0.18	M162_0.6	TAAGCGAT	0.42	.
CCGCCATT	0.18	.	GCTCCGAC	0.18	.	**CTAAG**CGG	0.42	.
CGGCCATT	0.18	.	AGATATTT	0.19	.	GCGATGTG	0.43	.
GCGGCCAT	0.19	.	**CTAAG**CGC	0.19	.	GCGGTGTG	0.43	.
GGGCGGCC	0.21	M151_0.6	GCTCTGAC	0.20	.	**CTAAG**CGA	0.46	.

Supplemental Table S5: The ten most positive and negative 8-mers from the 11 data sets. For each of the trained MTSA models, we identified the ten most positive and negative 8-mers. Matched RBP motif IDs from the CISBP-RNA database (FIMO with p-value $<10^{-3}$) are shown in the RBP column. Sequences matched to left and right flanking sequences are bolded and underlined, respectively.

Data set ID	Model without flanking sequences	Model with flanking sequences	Difference in Correlation
Mel12	0.46	0.54	+0.08
Khe13	0.41	0.44	+0.03
Khe13K	0.51	0.66	+0.15
Kwa14	0.46	0.56	+0.10
Ern16	0.44	0.49	+0.05
Ern16K	0.37	0.56	+0.19
Tew16	0.53	0.56	+0.03
Uli16	0.63	0.71	+0.08
Ino17	0.63	0.68	+0.05
Ino17W	0.54	0.58	+0.04
Kle20.HSS	0.44	0.51	+0.07
Kle20.ORI	0.49	0.57	+0.08
Kle20.pGL4	0.20	0.27	+0.07
Kle20.33MT	0.055	0.085	+0.03
Kle20.33WT	0.18	0.21	+0.03
Kle20.53MT	0.15	0.23	+0.08
Kle20.53WT	0.22	0.29	+0.07
Kle20.55MT	0.16	0.20	+0.04
Kle20.55WT	0.30	0.38	+0.08

Supplemental Table S6: Adding flanking sequences to tags significantly improves model performance. MTSA models were retrained by removing flanking sequences. The correlation between the observed relative expression and the predicted expression by these models are shown in the 2nd column. The correlation values in the 3rd column are the same as the *r* values shown in **Fig. 2A**, **Supplemental Fig. S2**, and **Supplemental Fig. S3**. Differences in the correlations are shown in the 4th column.

Data set ID	Minimum DNA count per tag (-m)	Minimum number of tags per CRE (-t)	Left flanking sequence (-l)	Right flanking sequence(-r)	Number of tags in training
Mel12	1,000	5	CTAGA	AGATC	12,689
Khe13/Khe13K	500	5	CTAGA	AGATC	25,344
Ern16/Ern16K	2,000	5	CTAGA	AGATC	10,127
Uli16	100	5	CTAGA	AGATC	63,977
Tew16	60	10	CTAGA	AGATC	72,435
Tew16N	60	10	CTAGA	AGATC	72,402
Kwa14	N/A	4	ATGCC	TGAGC	12,776
Mog13	N/A	4	.	.	2,436
Ino17	50	10	AATTC	CATTG	65,360
Ino17W	50	10	AATTC	CATTG	64,189
Kle20	.	10	CTAAG	CATTG	28,187

Supplemental Table S7: List of specific parameters for building MTSA training sets. For each of the data sets, we optimized the parameters as shown above to process and build MTSA training sets. For the Kle20 data set, we used a count per million (CPM) > 3 as a minimum DNA count.

Data set ID	RBP	miRNA
Mel12	47	0
Khe13	42	7
Khe13K	40	7
Ern16	44	5
Ern16K	42	4
Uli16	42	7
Tew16	81	20
Kwa14	36	9
Ino17	45	11
Kle20	56	19

Supplemental Table S8: Number of miRNA and RBP features selected for multivariate regression analyses. For each of the data sets, we selected miRNA and RBP that are likely to affect tag expression based on their expression and match frequencies in tags.

Supplemental Notes

While the original study (Ulirsch et al. 2016) reported 32 functional variants, we found 29 additional variants using the same data set and pipeline scripts. After consulting with the authors of the study, we discovered that the Quantile-Normalization step was not applied to the control data set in the published work. We therefore used the updated quantile normalized data. The original authors verified this issue and agreed with the usage of the updated results.